

Ab initio calculation of the ${}^4\text{He}(e, e'd)d$ reaction

D. Andreasi^{1,2}, S. Quaglioni^{1,2,a}, V.D. Efros³, W. Leidemann^{1,2,b}, and G. Orlandini^{1,2}

¹ Dipartimento di Fisica, Università di Trento, I-38050 Povo, Italy

² Istituto Nazionale di Fisica Nucleare, Gruppo Collegato di Trento, I-38050 Povo, Italy

³ Russian Research Centre “Kurchatov Institute”, 123182 Moscow, Russia

Received: 25 October 2005 / Revised version: 24 January 2006 /

Published online: 23 February 2006 – © Società Italiana di Fisica / Springer-Verlag 2006

Communicated by V. Vento

Abstract. The two-body knock-out reaction ${}^4\text{He}(e, e'd)d$ is calculated at various momentum transfers. The full four-nucleon dynamics is taken into account microscopically both in the initial and the final states. As NN interaction the central MT-I/III potential is used. The calculation shows a strong reduction of the coincidence cross-section due to the final-state interaction. Nonetheless, the theoretical results exhibit a considerable overestimation of the experimental cross-section at lower momentum transfer. Comparisons with other, less complete, calculations suggest that consideration of a more realistic ground state might not be sufficient for a good agreement with experiment, rather a more realistic final-state interaction could play an essential role.

PACS. 21.45.+v Few-body systems – 25.30.Fj Inelastic electron scattering to continuum – 27.10.+h $A \leq 5$

1 Introduction

Electron-induced two-body knock-out reactions are considered to be an important tool to investigate nucleon-nucleon (NN) correlations in nuclei. In comparison to one-nucleon knock-out processes two-nucleon emission reactions give more detailed information on NN dynamics, while many important details are already integrated out in the former case. Hence, quite a number of experimental and theoretical studies have been devoted to $(e, e'NN)$ reactions in order to study NN correlations (see, *e.g.*, [1]). However, it is often not very easy to obtain a clear picture of the two-body correlations, in fact one would need theoretical calculations where all relevant effects contributing to the observable under investigation are taken into account. For this reason in many theoretical works also effects from final-state interaction (FSI), as well as meson exchange and Δ currents have been considered. Microscopic calculations of two-body knock-out reactions with the proper final continuum state have only been carried out for two- and three-nucleon systems (see, *e.g.*, [2,3]). In more complex nuclei such exact and consistent studies are still missing.

The aim of the present paper is as follows. We want to consider the full FSI in a two-body emission reaction

microscopically and at the same time go beyond the above-mentioned two- and three-nucleon systems. To this end, we consider the ${}^4\text{He}(e, e'd)d$ reaction. The choice of this particular reaction is based on three different considerations. The first is that, differently from the two- and three-body systems, ${}^4\text{He}$ has some characteristics (binding energy per nucleon, density) rather similar to those of heavier nuclei. Secondly, the $(e, e'd)$ reaction has been suggested as a particularly useful tool for investigating short-range correlations (for a brief summary see [4]). In fact, the ${}^4\text{He}(e, e'd)d$ reaction was among the first NIKHEF experiments dedicated to the study of NN correlations [5]. The third reason is that in ref. [6] large effects of FSI were found in a two-deuteron cluster model. In this cluster model a phenomenological $d-d$ potential was used in order to describe the final-state interaction. Different from our calculation, in a deuteron cluster model channel mixing in the final state cannot be taken into account. We should mention that in ref. [7] it was suggested that channel mixing might be important for a correct theoretical description of the NIKHEF experiment [5].

In the present paper we perform a rigorous calculation of the FSI of the four-nucleon system, where the nucleons interact via an NN potential. We employ an integral transform method as outlined in ref. [8]. Particularly suited for such kind of calculations is the Lorentz Integral Transform (LIT), which was proposed in ref. [9]. In fact, the LIT has already been used for the calculation of var-

^a Present address: Department of Physics, P.O. Box 210081, University of Arizona, Tucson, Arizona 85721, USA.

^b e-mail: leideman@science.unitn.it

ious exclusive reactions: $d(e, e'p)n$ [10], ${}^4\text{He}(\gamma, p){}^3\text{H}$ [11], ${}^4\text{He}(\gamma, n){}^3\text{He}$ [11] and ${}^4\text{He}(e, e'p){}^3\text{H}$ [12].

Our paper is organized as follows. In sect. 2 we describe the formalism of the ${}^4\text{He}(e, e'd)d$ cross-section. A discussion of results and a short conclusion are given in sect. 3.

2 Formalism

The longitudinal part of the ${}^4\text{He}(e, e'd)d$ coincidence cross-section is given by

$$\frac{d^5\sigma_L}{de_k'd\Omega_{e'}d\Omega_d} = \sigma_M \frac{M_d p_d}{2(1 - (q/2p_d)\cos(\theta_d))} \frac{q_\mu^4}{q^4} F_L(\omega, q, \theta_d). \quad (1)$$

We do not consider other cross-section parts, where the transverse current is involved. The reason is that we intend to compare our results to the data of ref. [5]. In [6] it was shown that for the kinematics of that experiment the transverse current contributions to the cross-section are small. Such a result had to be expected and the smallness of the transverse contribution should be valid in general. The reason is that the leading transverse multipoles, *i.e.* electric and magnetic dipoles ($E1, M1$), are suppressed. In fact the ${}^4\text{He}(e, e'd)d$ reaction is of isoscalar nature (both ${}^4\text{He}$ and d have isospin 0). The unretarded $E1$ operator does not induce isoscalar transitions (isoscalar retardation effects are negligible at the rather small energy transfer for the $(e, e'd)$ reaction of [5]). Also the low-energy $M1$ operator is mainly isovector (sum of proton and neutron magnetic moments is small). On the contrary, for the leading longitudinal multipole, *i.e.* the Coulomb monopole in case of the NIKHEF kinematics, there is no such a suppression. In eq. (1) $e_{k'}$ and $\Omega_{e'}$ denote the energy and the solid angle of the scattered electron, and σ_M is the Mott cross-section. Energy and momentum transfer to the nuclear system are denoted by ω and $\mathbf{q} = q\hat{\mathbf{q}}$, q_μ^2 is the squared four-momentum transfer, θ_d denotes the angle between $\mathbf{p}_d = p_d\hat{\mathbf{p}}_d$, the outgoing deuteron momentum, and \mathbf{q} , while M_d is the deuteron mass. Note that for given values of ω , q , and p_d there is a unique deuteron knock-out angle, θ_d . The quantity $F_L(\omega, q, \theta_d)$ is the longitudinal structure function, defined as

$$F_L(q, \omega, \theta_d) = (G_E^p(q_\mu^2))^2 \sum_{M, M'} |\langle \Psi_{MM'}^-(E_{d,d}) | \hat{\rho}(\mathbf{q}) | \Psi_\alpha \rangle|^2. \quad (2)$$

Here $\Psi_{MM'}^-$ is the internal continuum final state of the minus type pertaining to the $d-d$ channel with a given relative momentum of the final $d-d$ pair (denoted below by \mathbf{k}) and deuteron spin projections M and M' . The quantity $E_{d,d}$ denotes the excitation energy of the four-nucleon system,

$$E_{d,d} = \epsilon_{d,d} - 2E_d + E_\alpha \quad \text{with} \quad \epsilon_{d,d} = \frac{k^2}{M_d}, \quad (3)$$

where E_d is the deuteron binding energy and E_α is the ${}^4\text{He}$ binding energy. The four-body ground state is denoted by

Ψ_α , and G_E^p is the proton electric form factor. As nuclear charge operator $\hat{\rho}$, we take

$$\hat{\rho}(\mathbf{q}) = \sum_{j=1}^4 \frac{1 + \tau_j^3}{2} \exp(i\mathbf{q} \cdot \mathbf{r}_j). \quad (4)$$

Here τ_j^3 denotes the third component of the j -th nucleon isospin and \mathbf{r}_j represents the position of the j -th nucleon with respect to the center of mass of the four-body system.

In our calculation we do not make use of the continuum wave function $\Psi_{MM'}^-$, but instead determine $F_L(q, \omega, \theta_d)$ by means of the integral transform method for exclusive reactions [8] with the Lorentz kernel [9,10]. In this approach one avoids to treat a continuum state problem, one works instead with a much easier bound-state-like problem. Our calculation is carried out in complete analogy to the ${}^4\text{He}(\gamma, p){}^3\text{H}$ and ${}^4\text{He}(e, e'p){}^3\text{H}$ calculations of [11,12], thus, in the following, we give only a very brief summary of the method.

The starting point of the calculation are the transition matrix elements

$$T_{MM'}(E_{d,d}) = \langle \Psi_{MM'}^-(E_{d,d}) | \hat{\rho} | \Psi_\alpha \rangle. \quad (5)$$

They can be divided into a Born term,

$$T_{MM'}^{\text{Born}}(E_{d,d}) = \langle \phi_{MM'}^-(E_{d,d}) | \hat{\mathcal{A}} \hat{\rho} | \Psi_\alpha \rangle, \quad (6)$$

and a FSI-dependent term,

$$T_{MM'}^{\text{FSI}}(E_{d,d}) = \left\langle \phi_{MM'}^-(E_{d,d}) \left| \mathcal{V} \hat{\mathcal{A}} \frac{1}{E_{d,d} + i\varepsilon - H} \hat{\rho} \right| \Psi_\alpha \right\rangle. \quad (7)$$

In the above two equations $\phi_{MM'}^-$ is a product of the internal wave functions of the two deuterons, with spin projections M and M' , and of the Coulomb function for their relative motion with a given large-distance momentum. The relative motion occurs in the average $d-d$ Coulomb potential. The potential \mathcal{V} is the sum of all interactions between nucleons belonging to different deuterons with the average $d-d$ Coulomb potential being subtracted, H denotes the full Hamiltonian of the four-nucleon system, and

$$\hat{\mathcal{A}} = \frac{1}{\sqrt{6}} (1 - P_{\alpha\gamma} - P_{\alpha\delta} - P_{\beta\gamma} - P_{\beta\delta} + P_{\alpha\gamma, \beta\delta}) \quad (8)$$

is an antisymmetrization operator, where P_{ij} is the permutation operator for particles i and j and $P_{ij,kl}$ permutes the particle pair (ij) with the pair (kl) . For any i and j one has

$$P_{ij} \hat{\mathcal{A}} \phi_{MM'}^-(\alpha\beta; \gamma\delta) = -\hat{\mathcal{A}} \phi_{MM'}^-(\alpha\beta; \gamma\delta), \quad (9)$$

where $\phi_{MM'}^-(\alpha\beta; \gamma\delta)$ is the final $d-d$ state with one deuteron consisting of pair $(\alpha\beta)$ and spin projection M and the second deuteron consisting of pair $(\gamma\delta)$ and spin projection M' . The calculation of the Born term is rather unproblematic and leads to the so-called plane-wave impulse approximation (PWIA) result. The FSI term is

much more complicated and is calculated with the integral transform method. To this end, first, the following identity:

$$\begin{aligned} T_{MM'}^{FSI}(E_{d,d}) &= \int_{E_{th}^-}^{\infty} \frac{F_{MM'}(E)}{E_{d,d} + i\varepsilon - E} dE \\ &= -i\pi F_{MM'}(E_{d,d}) + \mathcal{P} \int_{E_{th}^-}^{\infty} \frac{F_{MM'}(E)}{E_{d,d} - E} dE, \end{aligned} \quad (10)$$

is used, where E_{th} is the break-up threshold energy of ${}^4\text{He}$ in the isospin $T = 0$ channel and

$$\begin{aligned} F_{MM'}(E) &= \sum \int d\nu \langle \phi_{MM'}^-(E_{d,d}) | \mathcal{V} \hat{\mathcal{A}} | \Psi_\nu(E_\nu) \rangle \\ &\quad \times \langle \Psi_\nu(E_\nu) | \hat{\rho} | \Psi_\alpha \rangle \delta(E - E_\nu). \end{aligned} \quad (11)$$

The function $F_{MM'}$ contains information on all the eigenstates Ψ_ν for the whole eigenvalue spectrum of H . In the LIT method it is obtained by its Lorentz integral transform

$$\begin{aligned} L[F_{MM'}](\sigma) &= \int_{E_{th}^-}^{\infty} \frac{F_{MM'}(E)}{(E - \sigma_R)^2 + \sigma_I^2} dE \\ &= \langle \tilde{\Psi}_2(\sigma) | \tilde{\Psi}_1(\sigma) \rangle, \end{aligned} \quad (12)$$

where

$$\tilde{\Psi}_1(\sigma) = (H - \sigma)^{-1} \hat{\rho} | \Psi_\alpha \rangle, \quad (13)$$

$$\tilde{\Psi}_2(\sigma) = (H - \sigma)^{-1} \hat{\mathcal{A}} \mathcal{V} | \phi_{MM'}^-(E_{d,d}) \rangle \quad (14)$$

and $\sigma = \sigma_R + i\sigma_I$. Equation (12) shows that $L[F_{MM'}](\sigma)$ can be calculated without explicit knowledge of $F_{MM'}$, provided that one solves the two equations

$$(H - \sigma) | \tilde{\Psi}_1 \rangle = \hat{\rho} | \Psi_\alpha \rangle, \quad (15)$$

$$(H - \sigma) | \tilde{\Psi}_2 \rangle = \hat{\mathcal{A}} \mathcal{V} | \phi_{MM'}^-(E_{d,d}) \rangle. \quad (16)$$

The quantities $\tilde{\Psi}_1$ and $\tilde{\Psi}_2$ have finite norms and thus only bound-state techniques are required to obtain the solutions of eqs. (15) and (16).

We use expansions over a basis set of localized functions consisting of correlated hyperspherical harmonics (CHH) multiplied by hyperradial functions, which lead to rather large Hamiltonian matrices. Instead of using a time-consuming inversion method we directly evaluate the scalar products in (12) with the Lanczos technique as explained in ref. [13].

After having calculated $L[F_{MM'}](\sigma)$ one obtains the function $F_{MM'}(E)$, and thus $T_{MM'}(E_{d,d})$, via the inversion of the LIT. We perform the inversion as described in [14] (for other inversion methods, see [15]).

3 Results

In our calculation we use the semi-realistic MT-I/III potential [16] as NN interaction. This potential acts in the

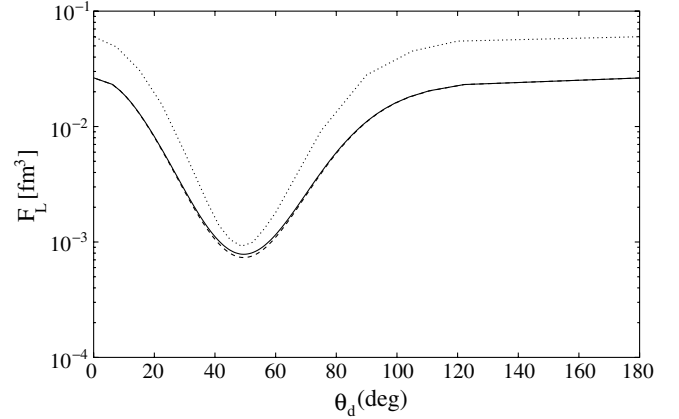


Fig. 1. Angular distribution of F_L at $\epsilon_{d,d} = 35$ MeV and $q_\mu^2 = 4.79$ fm $^{-2}$ without any FSI (dashed curve) and with inclusion of Coulomb-FSI (full curve); also shown the PWIA result of [4] (dotted curve).

even NN states ($S = 0, T = 1$ and $S = 1, T = 0$), while there is no interaction in the odd NN states ($S = 0, T = 0$ and $S = 1, T = 1$). Below pion threshold the MT-I/III potential leads to rather good descriptions of the NN s -wave phase shifts 3S_1 and 1S_0 . The Coulomb interaction is considered in addition. As already mentioned, the ground state of ${}^4\text{He}$ as well as $\tilde{\Psi}$ of eqs. (15) and (16) are calculated using the CHH expansion method. In order to speed up the convergence, state-independent correlations are introduced as in [17] (our ${}^4\text{He}$ wave function is identical with the CHH Ψ_α of [18]). The deuteron ground-state wave function is determined by a numerical solution of the radial Schrödinger equation. As proton electric form factor we take the usual dipole parametrization. The transition matrix elements (6) and (7) are calculated in the form of partial-wave expansions. For the Born term we take into account multipoles up to order $L = 20$, while for the FSI term we include multipoles up to $L = 5$. We checked that with such an expansion a sufficient convergence is reached.

In this work we consider the ${}^4\text{He}(e, e'd)$ reactions measured in the above-mentioned NIKHEF experiment [5]. This corresponds to the following kinematical settings: relative energy of the two final deuterons $\epsilon_{d,d} = 35$ MeV, missing momentum range $100 \text{ MeV}/c \leq |\mathbf{p}_m| \leq 150 \text{ MeV}/c$ ($\mathbf{p}_m = \mathbf{q} - \mathbf{p}_d$), and four-momentum transfers $q_\mu^2 = 1.75, 2.49, 3.36$ and 4.79 fm $^{-2}$.

We start our discussion considering the effect of the Coulomb FSI. In fig. 1 results are shown for the highest of the four considered momentum transfers. As one may expect the effect is very small and only visible in the cross-section minimum around $\theta_d = 50$ degrees. Similarly, small effects of the Coulomb FSI are found for the other three momentum transfers. Also shown in fig. 1 is the PWIA result of [4], where a harmonic oscillator (HO) s -state wave function is taken for the ${}^4\text{He}$ ground state, this ground state as well as the deuteron ground states are the only differences to our PWIA calculation (dashed curve). Although such a ground-state model is rather different from ours, one finds rather similar results in both calculations

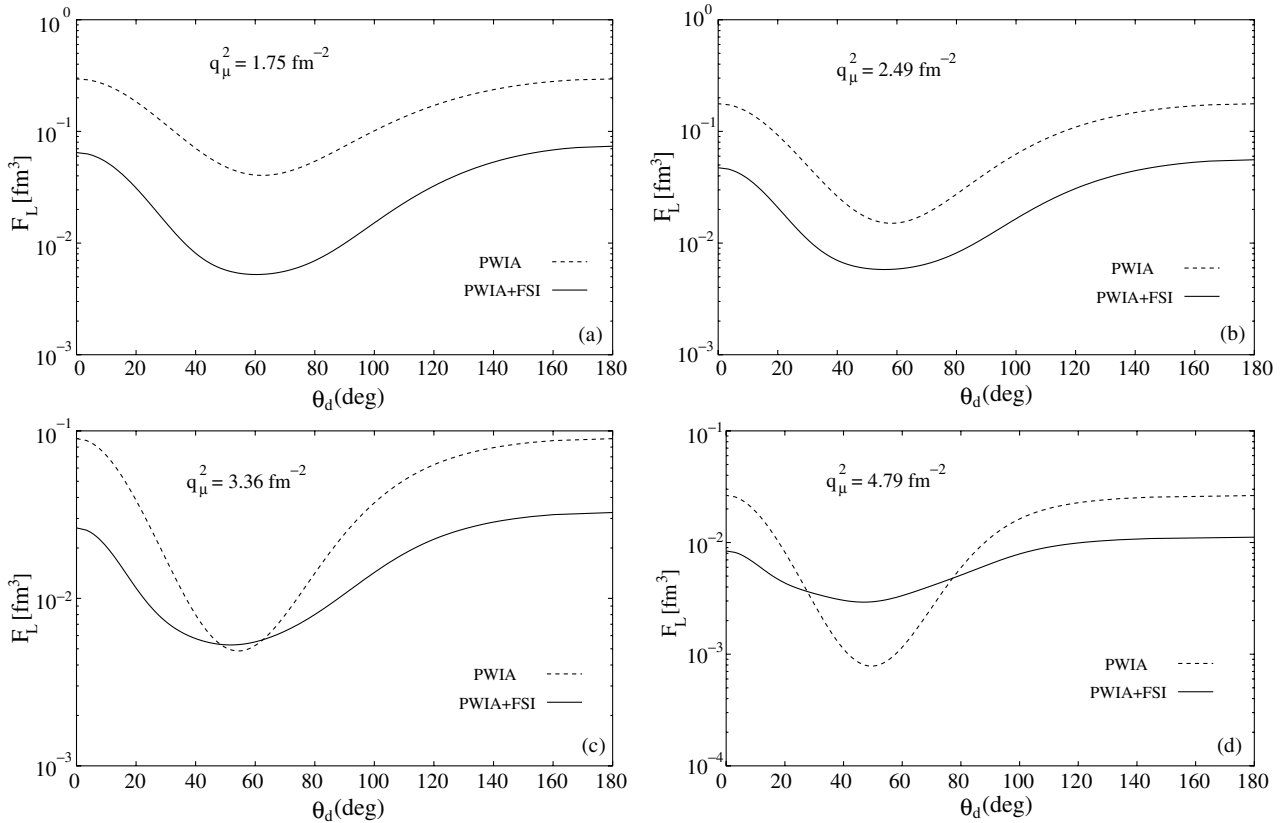


Fig. 2. Angular distribution of F_L with (full curve) and without (dashed curve) FSI contribution at $\epsilon_{d,d} = 35$ MeV and momentum transfers as indicated in the figure.

for the cross-section minimum, while at forward and backward angles the HO ground state leads to an increase of the cross-section by about a factor of two.

In fig. 2 we illustrate the effect of the full FSI for all four considered momentum transfers. Though the positions of the minima at about 50 degrees are hardly changed, it is readily evident that FSI is very important for all four considered momentum transfers. For the lower two q -values one obtains reductions of strength by about a factor of 5, while the shapes of the angular distribution remain almost unchanged. On the contrary, for the two higher momentum transfers also the shape is affected. One finds stronger decreases of F_L only in the forward region and for deuteron angles beyond 100 degrees and accordingly much less pronounced minima.

In fig. 3 we show the differential cross-section resulting from the calculated F_L at $q_\mu^2 = 4.79$ fm⁻². Different from the PWIA case the calculation with inclusion of FSI does not exhibit a minimum, but shows a rather constant fall-off with increasing deuteron knock-out angle. As already seen in fig. 2 the cross-section is significantly reduced by FSI for forward directions and beyond 100 degrees. In comparison to the experimental cross-section at $\theta_d \simeq 15$ degrees one finds for the PWIA an overestimation by about a factor of 2.6 and an underestimation by about a factor of 1.7 for the full calculation.

In fig. 4 we make a comparison of our results with experimental data also for the other considered momen-

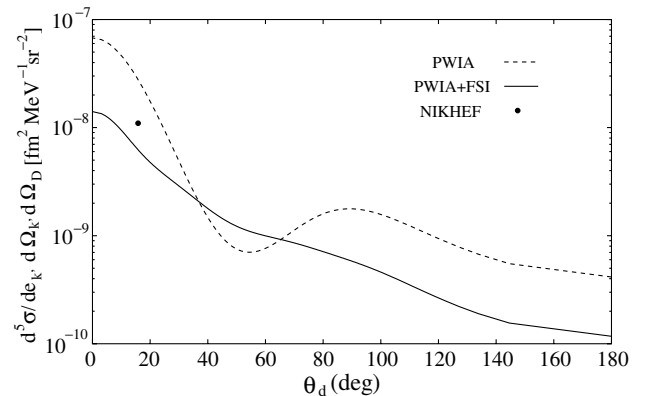


Fig. 3. Angular distribution of differential cross-section at $\epsilon_{d,d} = 35$ MeV and $q_\mu^2 = 4.79$ fm⁻² with (full curve) and without (dashed curve) FSI; also shown the experimental result from [5] (dot).

tum transfers. One sees that the rather strong reductions of the cross-sections due to FSI is by far not sufficient for an agreement with experiment at the lower momentum transfers. In fact the disagreement with experiment becomes more and more pronounced with decreasing momentum transfer. For the lowest q -value the experimental cross-section is overestimated by almost an order of magnitude. We mention again that an inclusion of the here not considered transverse current contributions should not

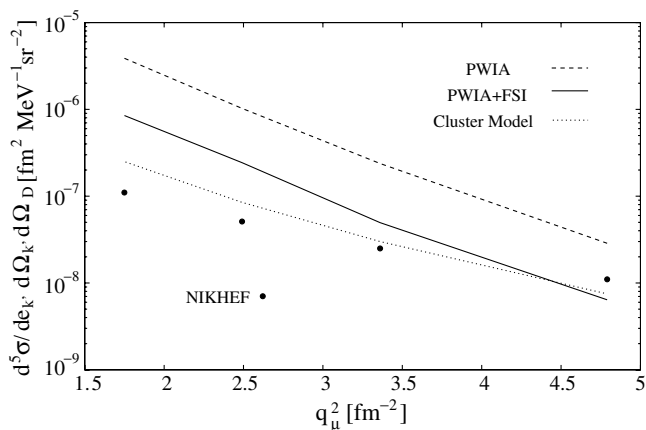


Fig. 4. Differential cross-section at $\epsilon_{d,d} = 35$ MeV and averaged over $100 \text{ MeV} \leq |\mathbf{p}_m| \leq 150 \text{ MeV}/c$ as function of q_μ^2 with (full curve) and without FSI (dashed curve) in comparison to experimental data (dots) [5]; also shown results from [6] with an HO ${}^4\text{He}$ ground state and FSI in a d - d cluster model for $|\mathbf{p}_m| = 125 \text{ MeV}/c$ (dotted curve).

lead to significant changes. In fact in ref. [6] it was shown that the one-body current increases the PWIA result by less than 20% for the lower three-momentum transfers and by about 25% for $q_\mu^2 = 4.79 \text{ fm}^{-2}$. Additional two-body currents are expected to be small because of the isoscalar nature of the ${}^4\text{He}(e, e'd)d$ reaction. In fig. 4 we also show theoretical results from [6] (note that the calculation of [6] is made for $|\mathbf{p}_m| = 125 \text{ MeV}/c$ and thus the cross-section has not been averaged over the experimental range $100 \leq |\mathbf{p}_m| \leq 150 \text{ MeV}/c$, we checked that the difference is not important). A considerably smaller discrepancy between theory and experiment is found than in our calculation. It should be pointed out that in [6] FSI is not calculated microscopically as in our case, but modelled via a central phenomenological potential between the two outgoing deuterons. As already mentioned the ${}^4\text{He}$ ground state of [6] is a simple harmonic-oscillator wave function.

In order to better understand the origin of the differences between the two calculations we show in fig. 5 the corresponding PWIA results. One notices that a large part of the differences of fig. 4 are already found for the PWIA results and thus are caused by the different ground-state wave functions. In the figure we also illustrate the PWIA calculation of Morita taken from [6], where correlations are introduced in the ${}^4\text{He}$ ground state via the ATMS method [19]. The ATMS and HO results are rather similar and considerably lower than ours below $q_\mu^2 = 2.5 \text{ fm}^{-2}$. The different results show that it is not very likely that a fully realistic calculation of the ${}^4\text{He}$ ground state could close the gap to experiment at lower momentum transfer. Most probably one needs a more realistic description of the FSI for the four-nucleon final state. It should be noted that the FSI effects of the present work and those of [6] are not very different, in fact in both cases one finds similar reductions of the corresponding PWIA cross-sections. However, we want to emphasize again that there are principal differences for the treatment of FSI in both calcula-

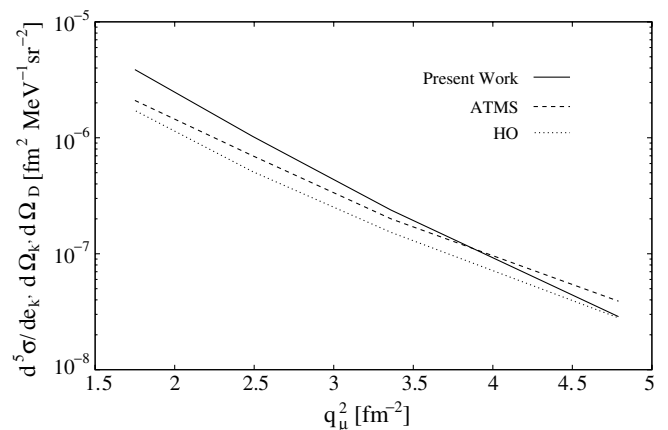


Fig. 5. Various PWIA results for the differential cross-section (kinematics as in fig. 4, but with $|\mathbf{p}_m| = 125 \text{ MeV}/c$): present work (full curve), HO [6] (dotted curve), and Morita's ATMS from [6] (dashed curve).

tions. On the other hand, both FSI calculations have in common that only central potentials between nucleons or, respectively, deuterons are taken into account. Probably, a consideration of tensor and other realistic force terms could change the picture significantly.

We summarize our work as follows. We have calculated the ${}^4\text{He}(e, e'd)d$ reaction taking into account the full four-nucleon dynamics in initial and final states. Such two-body knock-out reactions are considered as an excellent tool to determine two-body ground-state correlations. In fact the comparison of our PWIA results with corresponding results from other calculations show a non-negligible sensitivity of the cross-section to ground-state correlations. On the other hand, we find that FSI effects are even more important leading to a strong reduction of the cross-section. We thus confirm similar results from ref. [6], where, however, FSI was considered in a d - d cluster model only and not as in our case microscopically via a NN interaction. Compared to experimental data our theoretical results show deviations up to about 50% in the range $3.3 \text{ fm}^{-2} \leq q_\mu^2 \leq 4.8 \text{ fm}^{-2}$, but exhibit a considerable overestimation of the experimental cross-section at lower momentum transfers. As already pointed out a more realistic ${}^4\text{He}$ ground state will most likely not be sufficient for a satisfying improvement, whereas a more realistic nuclear interaction also for the final four-nucleon state might lead to an agreement of theoretical and experimental results. Admittedly the MT-I/III potential model is rather simple, but for the electromagnetic break-up of the three- and four-nucleon systems it has been shown that it leads generally to rather similar results than calculations with realistic nuclear forces (total photoabsorption cross-sections of ${}^3\text{H}/{}^3\text{He}$ [20] and of ${}^4\text{He}$ [18, 21, 22], ${}^3\text{H}/{}^3\text{He}(e, e')$ inelastic longitudinal form factors [23]). In addition, also for the ${}^4\text{He}(e, e')$ inelastic longitudinal form factor with the MT-I/III potential one finds a rather good agreement with experimental data [17]. However, in the present case with a final d - d state it might be possible that the tensor force in the final state plays a crucial role and thus a central potential model is insufficient.

References

1. A. Braghieri, C. Giusti, P. Grabmayr (Editors), *Proceedings of the 6th Workshop on Electromagnetically Induced Two-Hadron Emissions, Pavia 2003*, ISBN 88-85159-20-6 (2003).
2. H. Arenhövel, W. Leidemann, E.L. Tomusiak, Eur. Phys. J. A **23**, 147 (2005).
3. J. Golak, R. Skibinski, H. Witala, W. Glöckle, A. Nogga, H. Kamada, Phys. Rep. **415**, 89 (2005).
4. W. Leidemann, G. Orlandini, M. Traini, E. L. Tomusiak, Phys. Rev. C **50**, 630 (1994).
5. R. Ent, H. Blok, J.F.J. van den Brand, H.J. Bulten, E. Jans, L. Lapikas, H. Morita, Phys. Rev. Lett. **67**, 18 (1991).
6. W. Leidemann, G. Orlandini, M. Traini, E. Tomusiak, Phys. Lett. B **279**, 212 (1992).
7. R. Ent, B.L. Berman, H.P. Blok, J.F.J. van den Brand, W.J. Briscoe, M.N. Harakeh, E. Jans, P.D. Kunz, L. Lapikas, Nucl. Phys. A **578**, 93 (1994).
8. V.D. Efros, Yad. Fiz. **41**, 1498 (1985) (Sov. J. Nucl. Phys. **41**, 949 (1985)); **62**, 1975 (1999) (Phys. Atom. Nucl. **62**, 1833 (1999)).
9. V. Efros, W. Leidemann, G. Orlandini, Phys. Lett. B **338**, 130 (1994).
10. A. La Piana, W. Leidemann, Nucl. Phys. A **677**, 423 (2000).
11. S. Quaglioni, W. Leidemann, G. Orlandini, N. Barnea, V.D. Efros, Phys. Rev. C **69**, 044002 (2004).
12. S. Quaglioni, V.D. Efros, W. Leidemann, G. Orlandini, Phys. Rev. C **72**, 064002 (2005).
13. M.A. Marchisio, N. Barnea, W. Leidemann, G. Orlandini, Few-Body Syst. **33**, 259 (2003).
14. V.D. Efros, W. Leidemann, G. Orlandini, Few-Body Syst. **26**, 251 (1999).
15. D. Andreasi, W. Leidemann, C. Reiss, M. Schwamb, Eur. Phys. J. A **24**, 361 (2005).
16. R.A. Malfliet, J. Tjon, Nucl. Phys. A **127**, 161 (1969).
17. V.D. Efros, W. Leidemann, G. Orlandini, Phys. Rev. Lett. **78**, 432 (1997).
18. N. Barnea, V.D. Efros, W. Leidemann, G. Orlandini, Phys. Rev. C **63**, 057002 (2001).
19. H. Morita, Y. Akaishi, H. Tanaka, Prog. Theor. Phys. **79**, 863 (1988).
20. V.D. Efros, W. Leidemann, G. Orlandini, E.L. Tomusiak, Phys. Lett. B **484**, 223 (2000).
21. V.D. Efros, W. Leidemann, G. Orlandini, Phys. Rev. Lett. **78**, 4015 (1997).
22. D. Gazit, S. Bacca, N. Barnea, W. Leidemann, G. Orlandini, nucl-th/0512038.
23. V.D. Efros, W. Leidemann, G. Orlandini, E.L. Tomusiak, Phys. Rev. C **69**, 044001 (2004).